ARTICLE

Optimal Internal Noise for Mammalian Circadian Oscillator

Zhi-wei Wang[a,b], Zhong-huai Hou[a*], Hou-wen Xin[a*]

a. Department of Chemical Physics, University of Science and Technology of China, Hefei 230026, China; b. Teda Bio-X Research Center, Tianjin University of Science and Technology, Tianjin 300457, China

(Dated: Received on June 7, 2006; Accepted on July 6, 2006)

Based on a deterministic mammalian circadian oscillator proposed recently, we have constructed the corresponding mesoscopic stochastic model, and studied the effect of internal noise on the genetic oscillations of such a system. It is found that the stochastic genetic oscillations can show best performance at an optimal internal noise level via a mechanism of internal noise stochastic resonance. Furthermore, it is found that there exists a moderate system size that makes the stochastic model show effective oscillation at more extended region than the deterministic description, which indicates enhanced robustness as the result of internal noise. The potential biological application of such an effect is also discussed.

Key words: Internal noise, Genetic oscillation, Mesoscopic size effect, Stochastic resonance, Chemical langevin equation

I. INTRODUCTION

The molecular and biological bases of circadian timing, which accounts for the sleep/wake cycle, have attracted considerable attention and led to rapidly evolving models of the underlying 'clockwork'. Recently, mathematical models provide insight into detailed properties of the circadian oscillation [1,2], i.e. some models describe the molecular processes in great detail [3]. In mammals, circadian oscillations are generated within single neurons by intersected negative/positive feedback loops [4]. The negative feedback loop, which mainly includes *per* and *cry* genes and corresponding proteins, is considered as an essential element in generating circadian oscillations [5]. Meanwhile, the positive feedback loop, which primarily involves $Bmal_1$ and $Rev\text{-}erb\alpha$ genes and their proteins, has been showing roles in enhancing robustness of *Drosophila* [6] and mutant mice [7].

At the molecular level, circadian oscillation is regulated by gene expression. It is well known that many regulatory molecules act at rather low concentration in the processes of gene expression, leading to large random fluctuations on the reaction rates of these processes [8]. Since Arkin and co-workers [9] realized that the reactions underlying gene expression occur in abrupt stochastic bursts rather than successive deterministic manner, it has been realized that in various systems the intrinsic noise of gene expression is inherent and should be paid considerable attention [10]. The effects of molecular fluctuations were shown to be prominent and can not be ignored in models of transcriptional regulation [11,12] and signal cascades [13]. Up to now, most of the studies accounting for the intrinsic noise in gene expression focus on how to measure, characterize and explain the intrinsic noise experimentally or theoretically, and how the system shows robustness to intrinsic noise by feedback loops or redundancy on viewing the noise as a nuisance.

However, some recent studies have explored the roles of noise in the dynamics of gene expression, such as intrinsic noise may induce oscillations which are not present in the deterministic model [14], or induce bifurcations which have no counterpart in the deterministic description [15]. Meanwhile, in some reverse engineering approaches, some regulatory mechanisms may exploit intrinsic noise to randomize outcomes where variability is advantageous [16]. In this way, the intrinsic noise can be used to control a toggle switch [17-19], or a repressilator, in which three gene products inhibit the transcription of each other in a cyclic way [20]. More importantly, among the studies where the intrinsic noise systematically facilitates the system properties, it was found that in a cellular control system intrinsic noise may enhance the sensitivity of intracellular regulation by stochastic focusing (SF) [13], and that in a genetic control circuit the fluctuations in repressor or corepressor numbers can improve the control of gene expression [21]. Interestingly, it was found that optimal internal noise effect exists in some sub-cellular system. Shuai and Jung demonstrated that optimal intracellular calcium signaling appears at a certain size or distribution of the ion channel clusters [22-24]. In previous studies, we have also found the constructive roles of internal noise or optimal system size effects in prokaryotic circadian clock system [25], calcium signaling system [26] and synthetic gene network [27]. However, few works so far account for the effect of internal noise in mammalian circadian clock system, in which the interlocked

*Author to whom correspondence should be addressed. E-mail: hzhlj@ustc.edu.cn, hxin@ustc.edu.cn

negative/positive feedback loops have great impact on system dynamics behavior.

In the present work, we use a recently proposed mammalian circadian model [28] and investigate the effect of internal noise on the genetic oscillations of such a system. The model accounts for the interdependence of the positive and negative feedback, and shows sustained oscillations in agreement with experimental observations with periods and phases. We first constructed the mesoscopic stochastic model from the original one; and then find that the stochastic genetic oscillations can show best performance at an optimal internal noise level via a mechanism of internal noise stochastic resonance (INSR). Furthermore, we find that there exists a moderate system size that makes the stochastic model show effective oscillation (EO) at more extended region than the deterministic description. Since the magnitude of the internal noise is determined by the system size, such phenomena also demonstrate some optimal system size effect. Finally we discuss some potential biological applications of such an optimal system size effect.

II. MODEL DESCRIPTION

The model proposed by Becker-Weimann *et al.* is a mammalian circadian core oscillator described by ordinary differential equations. The variables represent the concentration of clock genes' mRNAs and proteins. The deterministic dynamics is described by the following equations,

$$\begin{aligned}
\frac{\mathrm{d}y_1}{\mathrm{d}t} &= \frac{v_{1\mathrm{b}}(y_7+c)}{k_{1\mathrm{b}}[1+(y_3/k_{1\mathrm{i}})^p]+(y_7+c)} - k_{1\mathrm{d}}y_1 \\
\frac{\mathrm{d}y_2}{\mathrm{d}t} &= k_{2\mathrm{b}}y_1^q + k_{3\mathrm{t}}y_3 - k_{2\mathrm{t}}y_2 - k_{2\mathrm{d}}y_2 \\
\frac{\mathrm{d}y_3}{\mathrm{d}t} &= k_{2\mathrm{t}}y_2 - k_{3\mathrm{t}}y_3 - k_{3\mathrm{d}}y_3 \\
\frac{\mathrm{d}y_4}{\mathrm{d}t} &= \frac{v_{4\mathrm{b}}y_3^r}{k_{4\mathrm{b}}^r+y_3^r} - k_{4\mathrm{d}}y_4 \\
\frac{\mathrm{d}y_5}{\mathrm{d}t} &= k_{5\mathrm{b}}y_4 + k_{6\mathrm{t}}y_6 - k_{5\mathrm{t}}y_5 - k_{5\mathrm{d}}y_5 \\
\frac{\mathrm{d}y_6}{\mathrm{d}t} &= k_{5\mathrm{t}}y_5 + k_{7\mathrm{a}}y_7 - k_{6\mathrm{t}}y_6 - k_{6\mathrm{a}}y_6 - k_{6\mathrm{d}}y_6 \\
\frac{\mathrm{d}y_7}{\mathrm{d}t} &= k_{6\mathrm{a}}y_6 - k_{7\mathrm{a}}y_7 - k_{7\mathrm{d}}y_7
\end{aligned} \tag{1}$$

here y_1 to y_7 represent the concentrations of per_2 or cry mRNA, $\mathbf{PER_2/CRY}$ complex in the cytoplasm, $\mathbf{PER_2/CRY}$ complex in the nucleus, $Bmal_1$ mRNA, cytoplasmatic $\mathbf{BMAL_1}$ protein, $\mathbf{BMAL_1}$ protein in the nucleus and transcriptionally active form $\mathbf{BMAL_1}$*, respectively. The parameters starting with v denote the corresponding transcriptional maximal rates, and that starting with k denote the common reaction rates of the processes, such as transcription (with suffix b), import/export (with suffix t), activation (with suffix a) and degradation (with suffix d). p and r correspond to the hill coefficient of inhibition of per_2/cry transcription and activation of $Bmal_1$ transcription, respectively. q is the number of $\mathbf{PER_2/CRY}$ complex forming subunits. The essence of the model is the introduction of positive feedbacks that can modulate the dynamics of the system. Here the concentration of constitutive activator c and maximal rate of $Bmal_1$ transcription $v_{4\mathrm{b}}$ both account for the positive feedbacks, so we choose them as control parameters. The parameter values that remain unchanged during our simulation are listed in Table I. See [28] for more details.

The Eq.(1) is a rather good description of the deterministic dynamics. However, due to the small system size, one is wondering how the internal noise would affect the system's behavior. To account for the internal noise, such a deterministic description is not exactly valid and one can describe the reaction as a birth-death stochastic process governed by a chemical master equation. Generally, there is no practical procedure to solve chemical master equation analytically, but it still provides the basis for numerical simulation. One of the widely used simulation algorithm is exact stochastic simulation method introduced by Gillespie in 1977 [29], which stochastically determines what's the next reaction step and when it will happen according to the transition probability of each reaction event. This simulation method exactly accounts for the internal noise. For the present model, the 23 reaction steps drawn from the reaction details and the corresponding transition rates are listed in Table I, note that the transition rates are proportional to the system size V. Although the exact stochastic simulation method has been widely used to study the effects of internal noise in many systems, it is too time-consuming when the system size is large. Recently, Gillespie developed the τ-leap method [30] that randomly determines how many steps will take place for each reaction channel in the next "macro-infinitesimal" time interval τ. It has been proved that the τ-leap method is a rather good approximation of the exact method when the system size is large. Therefore, it is advisable for us to use the exact stochastic simulation method when the system size is small enough and employ the τ-leap method when the system size is too large for the exact stochastic simulation method.

In addition, a further alternative method to study the internal noise is chemical Langevin (CL) method, which was also proposed by Gillespie [31]. It was proved that the chemical Langevin equation (CLE) is a rather good approximation if a "macro-infinitesimal" time scale exists in the system. From the form of CLE one can easily see that the internal noise is related to the system size and the parameter values, as well as the state variables that evolve with time. To further facilitate the simulation and show robustness of our results, we have also performed studies based on the CLE. For the present model, the CLE reads

ISSN 1003-7713/DOI:10.1360/cjcp2007.20(2).119.7

TABLE I Reaction steps and corresponding transition rates involved in the model

Reaction steps	Descriptions	Transition rates
$Y_1 \to Y_1 + 1$	Generation of per_2 or cry mRNA	$W_1 = a_1 V$
$Y_1 \to Y_1 - 1$	Degradation of per_2 or cry mRNA	$W_2 = a_2 V = k_{1\mathrm{d}} Y_1$
$Y_2 \to Y_2 + 1$	Increment of $\mathbf{PER_2/CRY}$ complex in	$W_3 = a_3 V = k_{2\mathrm{b}}(Y_1/V)^q V$
	cytoplasm by formation and transportation	$W_4 = a_4 V = k_{3\mathrm{t}} Y_3$
$Y_2 \to Y_2 - 1$	Reduction of $\mathbf{PER_2/CRY}$ complex in	$W_5 = a_5 V = k_{2\mathrm{t}} Y_2$
	cytoplasm by transportation and degradation	$W_6 = a_6 V = k_{2\mathrm{d}} Y_2$
$Y_3 \to Y_3 + 1$	Increment of $\mathbf{PER_2/CRY}$ complex in nucleus by transportation	$W_7 = a_7 V = k_{2\mathrm{t}} Y_2$
$Y_3 \to Y_3 - 1$	Reduction of $\mathbf{PER_2/CRY}$ complex in nucleus	$W_8 = a_8 V = k_{3\mathrm{t}} Y_3$
	by transportation and degradation	$W_9 = a_9 V = k_{3\mathrm{d}} Y_3$
$Y_4 \to Y_4 + 1$	Generation of $Bmal_1$ mRNA	$W_{10} = a_{10} V$
$Y_4 \to Y_4 - 1$	Degradation of $Bmal_1$ mRNA	$W_{11} = a_{11} V = k_{4\mathrm{d}} Y_4$
$Y_5 \to Y_5 + 1$	Increment of cytoplasmatic $\mathbf{BMAL}_1$ protein	$W_{12} = a_{12} V = k_{5\mathrm{b}} Y_4$
	by formation and transportation	$W_{13} = a_{13} V = k_{6\mathrm{t}} Y_6$
$Y_5 \to Y_5 - 1$	Reduction of cytoplasmatic $\mathbf{BMAL}_1$ protein	$W_{14} = a_{14} V = k_{5\mathrm{t}} Y_5$
	by transportation and degradation	$W_{15} = a_{15} V = k_{5\mathrm{d}} Y_5$
$Y_6 \to Y_6 + 1$	Increment of $\mathbf{BMAL}_1$ protein in nucleus by	$W_{16} = a_{16} V = k_{5\mathrm{t}} Y_5$
	transportation and activation	$W_{17} = a_{17} V = k_{7\mathrm{a}} Y_7$
$Y_6 \to Y_6 - 1$	Reduction of $\mathbf{BMAL}_1$ protein in nucleus by	$W_{18} = a_{18} V = k_{6\mathrm{a}} Y_6$
	activating, transportation and degradation	$W_{19} = a_{19} V = k_{6\mathrm{t}} Y_6$
		$W_{20} = a_{20} V = k_{6\mathrm{d}} Y_6$
$Y_7 \to Y_7 + 1$	Increment of $\mathbf{BMAL}_1$* protein by activation	$W_{21} = a_{21} V = k_{6\mathrm{a}} Y_6$
$Y_7 \to Y_7 - 1$	Reduction of $\mathbf{BMAL}_1$* protein by activating and degradation	$W_{22} = a_{22} V = k_{7\mathrm{a}} Y_7$
		$W_{23} = a_{23} V = k_{7\mathrm{d}} Y_7$

here $a_1 = \dfrac{v_{1b}(y_7 + c)}{k_{1b}[1 + (y_3/k_{1i})^p] + (y_7 + c)}$ and $a_{10} = \dfrac{v_{4b} y_3^r}{k_{4b}^r + y_3^r}$. Parameter values that remain unchanged during simulation: $v_{1\mathrm{b}}$=9 nmol/Lh, $k_{1\mathrm{b}}$=1 nmol/L, $k_{1\mathrm{i}}$=0.56 nM, p=8, $k_{1\mathrm{d}}$=0.12 h^{-1}, $k_{2\mathrm{b}}$=0.3 nmol/L/h, q=2, $k_{2\mathrm{t}}$=0.24 h^{-1}, $k_{2\mathrm{d}}$=0.05 h^{-1}, $k_{3\mathrm{t}}$=0.02 h^{-1}, $k_{3\mathrm{d}}$=0.12 h^{-1}, $k_{4\mathrm{b}}$=2.16 nmol/L, r=3, $k_{4\mathrm{d}}$=0.75 h^{-1}, $k_{5\mathrm{t}}$=0.45 h^{-1}, $k_{5\mathrm{b}}$=0.24 h^{-1}, $k_{5\mathrm{d}}$=0.06 h^{-1}, $k_{6\mathrm{t}}$=0.06 h^{-1}, $k_{6\mathrm{a}}$=0.09 h^{-1}, $k_{6\mathrm{d}}$=0.12 h^{-1}, $k_{7\mathrm{a}}$=0.003 h^{-1}, $k_{7\mathrm{d}}$=0.09 h^{-1}.

$$
\begin{aligned}
\frac{\mathrm{d}y_1}{\mathrm{d}t} &= a_1 - a_2 + \frac{1}{\sqrt{V}}[\sqrt{a_1}\xi_1(t) - \sqrt{a_2}\xi_2(t)] \\
\frac{\mathrm{d}y_2}{\mathrm{d}t} &= a_3 + a_4 - a_5 - a_6 + \frac{1}{\sqrt{V}}[\sqrt{a_3}\xi_3(t) \\
&\quad + \sqrt{a_4}\xi_4(t) - \sqrt{a_5}\xi_5(t) - \sqrt{a_6}\xi_6(t)] \\
\frac{\mathrm{d}y_3}{\mathrm{d}t} &= a_7 - a_8 - a_9 + \frac{1}{\sqrt{V}}[\sqrt{a_7}\xi_7(t) - \sqrt{a_8}\xi_8(t) \\
&\quad - \sqrt{a_9}\xi_9(t)] \\
\frac{\mathrm{d}y_4}{\mathrm{d}t} &= a_{10} - a_{11} + \frac{1}{\sqrt{V}}[\sqrt{a_{10}}\xi_{10}(t) - \sqrt{a_{11}}\xi_{11}(t)] \\
\frac{\mathrm{d}y_5}{\mathrm{d}t} &= a_{12} + a_{13} - a_{14} - a_{15} + \frac{1}{\sqrt{V}}[\sqrt{a_{12}}\xi_{12}(t) \\
&\quad + \sqrt{a_{13}}\xi_{13}(t) - \sqrt{a_{14}}\xi_{14}(t) - \sqrt{a_{15}}\xi_{15}(t)] \\
\frac{\mathrm{d}y_6}{\mathrm{d}t} &= a_{16} + a_{17} - a_{18} - a_{19} - a_{20} + \frac{1}{\sqrt{V}}[\sqrt{a_{16}} \\
&\quad \xi_{16}(t) + \sqrt{a_{17}}\xi_{17}(t) - \sqrt{a_{18}}\xi_{18}(t) \\
&\quad - \sqrt{a_{19}}\xi_{19}(t) - \sqrt{a_{20}}\xi_{20}(t)] \\
\frac{\mathrm{d}y_7}{\mathrm{d}t} &= a_{21} - a_{22} - a_{23} + \frac{1}{\sqrt{V}}[\sqrt{a_{21}}\xi_{21}(t) \\
&\quad - \sqrt{a_{22}}\xi_{22}(t) - \sqrt{a_{23}}\xi_{23}(t)]
\end{aligned}
\tag{2}
$$

here a_1-a_{23} are the transition rates per volume listed in Table I, and ξ_1 to ξ_{23} is Gaussian white noise with zero mean $\langle \xi_i(t) \rangle$=0 and correlation of $\langle \xi_i(t)\xi_j(t') \rangle$=$\delta_{ij}\delta(t - t')$. Without the second terms in the brackets at the right side, the CLE (2) is equivalent with the deterministic Eq.(1). Therefore, these terms actually reflects the effects of the internal noise. It is quite clear that the magnitude of the internal noise items is proportional to $1/\sqrt{V}$, and they depend not only on the control parameter but also on the concentrations of mRNAs and proteins.

III. RESULTS AND DISCUSSION

A. Bifurcation properties

As already well known from numerous studies, noise often plays constructive roles near the bifurcation

ISSN 1003-7713/DOI:10.1360/cjcp2007.20(2).119.7

points. Guided by Fig.1 in [28] and set c and v_{4b} as control parameters, we perform numerical calculation of Eq.(1) using explicit Euler method with time step 0.001 h and parameters as listed in Table I and find that there exists 4 regions with different dynamics behavior, as plotted in Fig.2. See caption of Fig.2 for more details about the bifurcation properties. To study the system dynamics in a more simplified way, we take assumption that all variables initialized at 1, in which case the bifurcation diagram can be simplified as the inserted figure in Fig.2. One can see that for a fixed value of c, there exists only one Hopf bifurcation (HB) point of v_{4b}. In the present work, we focus on the effect of internal noise when the control parameters are tuned very close to the Hopf bifurcation. To this end, we first fix c at 0.005, and find that there exists a supercritical Hopf bifurcation point at about v_{4b}=0.51.

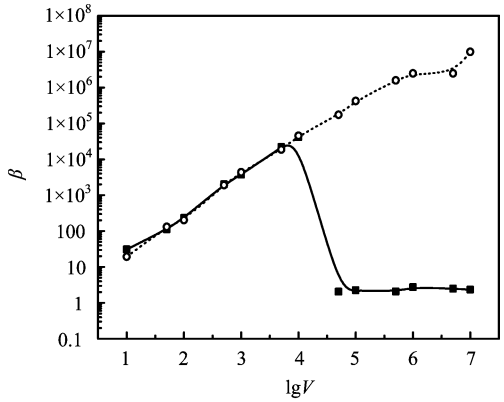

FIG. 1 The dependence of SNR on system size for c=0.0031 and v_{4b}=1.0 with different initial condition. Open circles: all variables initialized at 1, solid square: all variables initialized at 0.

If the system stays inside the steady-state region and we do not account for the internal noise, the system would not oscillate. But if the internal noise is taken into account, simulation results via the exact stochastic simulation method, the τ-leap method and the CLE, all show stochastic oscillations. Such stochastic oscillations do not solely contain random noisy information, for there are clear peaks in their power spectrums (Fig.3(a) and Fig.3(b)).

B. Internal noise stochastic resonance

The stochastic oscillation due to internal noise implies some kind of resonance effect. On one hand, there is no oscillation in the steady-state region when the internal noise is not taken into account. On the other hand, if the system size is too small, the internal noise becomes so large that sustained oscillation would be overwhelmed by random noise. Therefore, it can be predicted that for some intermediate system size and

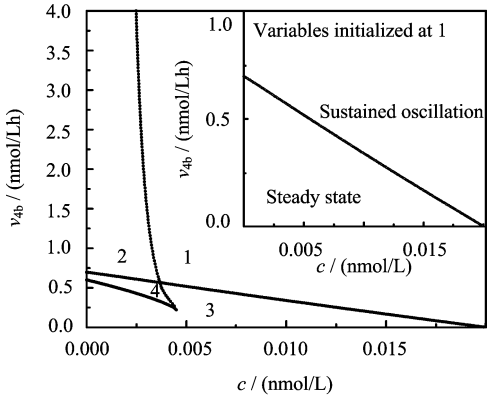

FIG. 2 The bifurcation diagram of the model. c and v_{4b} are both chosen as control parameters. The four parameter regions indicate different types of dynamical behavior. In region 1 the system shows oscillation; and the system stays at stable steady state in region 3. In region 2 and 4 the dynamics are somewhat complex in that more than one stable state coexists. In region 2, oscillations coexist with stable steady states, and whether the system show oscillation or steady state depends on the initial condition. For example, the systems of c=0.002 and v_{4b}=3.0 show oscillation when all variables initialized at 1 and show stable steady state when all variables initialized at 0. In region 4, two stable steady states coexist. See Ref.[28] for more details. The inserted figure is the bifurcation diagram when all variables initialized at 1. Here the difference between the two stable steady states is omitted.

corresponding internal noise level, the stochastic oscillation due to internal noise would be most pronounced.

To measure the relative performance of the stochastic oscillation quantitatively, we define an effective signal-to-noise ratio (SNR) β=$R/(\Delta\omega/\omega_p)$, where ω_p is the frequency at the peak, $\Delta\omega$ is the width between ω_p and the frequency ω_l satisfying ω_l>ω_p and $P(\omega_1)$= $P(\omega_p)/e$, here $P()$ denotes the power spectrum density (PSD) for a given frequency; R=$P(\omega_p)/P(\omega_2)$, where $P(\omega_2)$ is the smallest PSD value between $P(0)$ and $P(\omega_p)$. See also the caption of Fig.3(b) for more details. For the present model, the dependence of β on system size V for c=0.005 and v_{4b}=0.46 is plotted in Fig.3(c). The time series used to calculate the power spectrum contains 16,384 data points with an average time interval 0.3 h. The smoothed power spectrum curves are obtained by the nearest averaging over 50 points from the original ones. A Welch window function is used during the estimation of the power spectrum. One can see that a clear peak is present for system size $V\approx10^4$-10^5, which demonstrate the existence of a resonance effect. Since the resonance effect is caused by internal noise, it can be termed as internal noise stochastic resonance (INSR), reminiscent of the well-known phenomenon of stochastic resonance (SR) [32,33].

From Fig.3(c) one can see good qualitative agreement among the chemical Langevin method, the exact stochastic simulation method and the τ-leap method.

ISSN 1003-7713/DOI:10.1360/cjcp2007.20(2).119.7

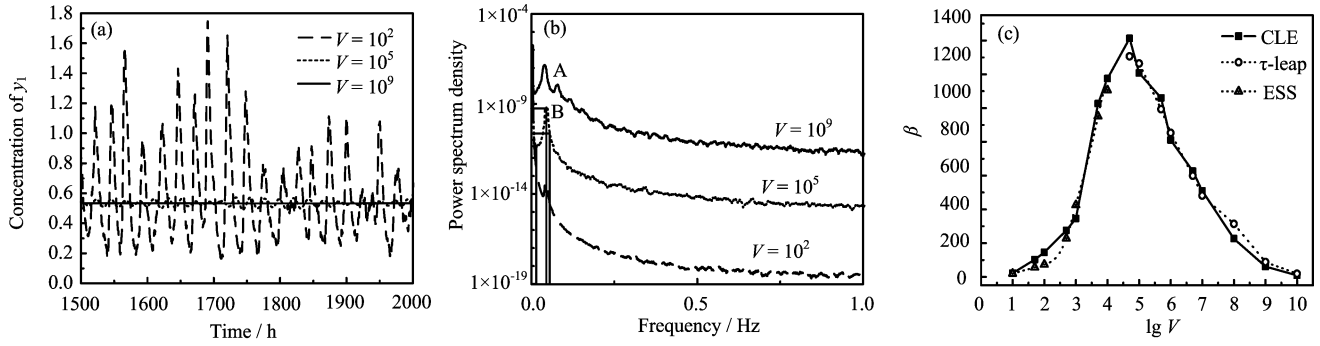

FIG. 3 (a) The stochastic oscillations of y_1 concentration for three system sizes V=10^2, 10^5 and 10^9, respectively. The control parameters are c= 0.005 and v_{4b}=0.46. The curve for V=10^2 is obtained from exact stochastic simulation method, while the other two are obtained by CL method. (b) Corresponding smoothed power spectrums for the time series in (a), respectively. The points A, B and C in the PSD curve demonstrate how to calculate the SNR value, β=$[P(B)/P(A)] \times \omega_B/(\omega_C - \omega_B)$, where point C is located by the condition $P(C)$=$P(B)/e$. (c) The dependency of SNR on the system size V for c=0.005 and v_{4b}=0.46. Open triangles: data obtained by exact stochastic simulation method for V<10^5, open circles: results from τ-leap method for $V \geq 10^5$, solid square: data from CL method.

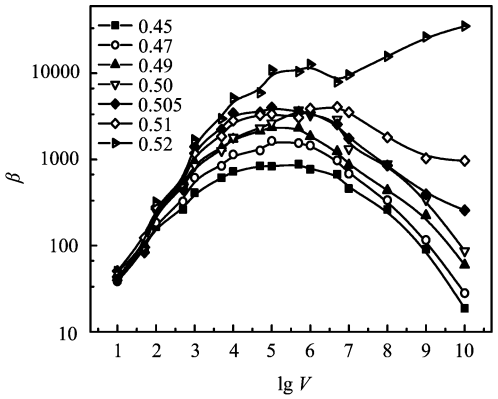

FIG. 4 The dependency of SNR on system size for different values of v_{4b} when c=0.005 by CL method. The curves are the nearest smoothed over 3 points from the original ones.

Such agreement implies that it is convenient to use the CLE to study the qualitative effects of internal noise in a systematic way. Using the CL method, we have also studied how the SR behavior depends on the value of the control parameter. The results of c=0.005 and several different v_{4b} value are shown in Fig.4. When the control parameter v_{4b} becomes closer to the Hopf bifurcation point, the SR curve becomes higher. One can see the optimal system sizes are always about $V \approx 10^4$-10^5. It is shown that for those v_{4b} slightly smaller than the Hopf bifurcation point, the internal noise can play a constructive role at a moderate system size. While for those v_{4b} slightly larger than the Hopf bifurcation point, the peak disappears and the SNR increases monotonically with the increment of system size. In this case, the internal noise due to small system size always play a destructive role.

C. Effective oscillation region

Oscillation is ubiquitous in biological systems. However, oscillations with very small amplitude are often useless in performing biologic functions for their poor ability on carrying and transferring signals. To study the properties of sustained oscillations due to internal noise, we define the oscillation whose effective SNR is larger than a threshold value as the effective oscillation (EO). In the present work, we set the threshold value of effective SNR as 500.0, which is the largest SNR value when the system size V=10^2.

Figure 5 shows our numerical results with three system size at different control parameter values of c and v_{4b}. Each point denotes the threshold value of v_{4b} that makes the EO occur with fixed c. One can see that when the system size is very large (V=10^9), the internal noise is so small that the EO boundary is very close to the deterministic one, which is composed of a

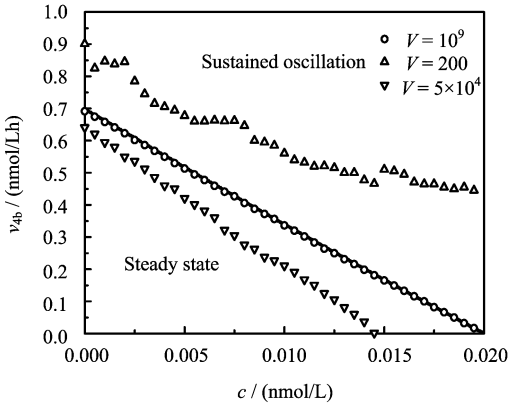

FIG. 5 EO boundaries for three system sizes when the variables c and v_{4b} are varied simultaneously. The area above the borderline is the EO region of that system size.

ISSN 1003-7713/DOI:10.1360/cjcp2007.20(2).119.7

series of Hopf bifurcation points. Furthermore, when the system size is too small (V=10^2), the internal noise is so large that the EO region is relatively small, only the points with large enough control parameters c and v_{4b} have the ability to resist the perturbation of internal noise. However, for a moderate system size (here V=5×10^4), the EO can even occur at the point that remains steady state in the deterministic description as the result of INSR. In this way, the area of EO can be enlarged and internal noise enhances robustness as a result of small system size.

D. Discussion

Our simulation is exerted near the supercritical Hopf bifurcation point of v_{4b} at a fixed c, where the system only shows a stable steady state when internal noise is not accounted for. However, once the internal noise is taken into account, internal periodic oscillation can be stimulated, so the sustained oscillation can be observed and it contains not only random signals but also the inherently system signal. Furthermore, the performance of such sustained oscillation undergoes a maximum with the increment of internal noise, which implies the occurrence of INSR. Such phenomenon is common in that for different value of c there always exists an optimal internal noise level. Previous studies on mammalian circadian clock system often ignore the effect of intrinsic noise, or view noise as a nuisance, so the regulatory mechanisms need to show resistance to random noise. However, in the present work, noise can play constructive roles via INSR such that the regulatory mechanism may exploit the advantage of internal noise. Furthermore, we find that there exists an optimal internal noise level that makes the stochastic model show EO at more extended region than the deterministic description. Since the magnitude of internal noise is determined by the system size, such INSR also demonstrates the existence of an optimal system size, and indicates the enlargement of the EO region as a result of small system size.

In this work, we use the initial condition of all variable initialized at 1 for simplification. In fact, it is not necessary for the occurrence of INSR. Most of our results can be repeated at all variables initialized at 0. Besides this, there are some different phenomena if all variables initialized at 0. As an example, we show in Fig.1 the different dynamics resulting from different initial condition. One can see that the SNRs for c=0.0031 and v_{4b}=1.0 increase monotonously with the increment of system size when all the variables are initialized at 1, while they undergo a maximum if all variables are initialized at 0. The bifurcation diagram Fig.2 can explain such phenomenon in that the deterministic state of the point is different for different initial condition (region 4).

It is now already known that many biological systems can take advantage of benefits of noise for nonlinear transmission and amplification of feeble information, and here we expanded such advantageous roles to a mammalian circadian system. In addition, from our results one can see the performance of sustained oscillation is optimal in $V\approx10^4$-10^5. Since the optimal system size exists in the present model, the biological organism may learn to adjust the kinetic parameters to make it work at an optimal size. Due to the complexity of mammal organism, the real cell size may be affected by many other factors, so our optimal system size by simulation might have deviation with the real size; however, we believe the deviation would not be too large. Since the process of circadian clock in mammals is of ubiquitous importance in biology, the optimal system size effect could be remarkable.

IV. CONCLUSION

In conclusion, we have constructed a mesoscopic stochastic model for a mammalian circadian clock core model, and studied the effect of internal noise on the genetic oscillations of such a system. We find that the stochastic genetic oscillations can show best performance at an optimal internal noise level via a mechanism of INSR. Since the magnitude of the internal noise is determined by the system size, this phenomenon also demonstrates the existence of an optimal system size. Furthermore, we find that the stochastic model show EO at more extended region than the deterministic description, which indicates enhanced robustness as a result of small system size. Our findings may find some interesting applications for gene regulatory processes *in vivo*.

V. ACKNOWLEDGMENTS

The authors were indebted to S. Becker-Weimann *et al.* for using their model. This work was supported by the National Natural Science Foundation of China (No.20673106 and No.20433050), the Author of National Excellent Doctoral Dissertation of PR China (FANEDD).

[1] A. Goldbeter, Nature **420**, 238 (2002).
[2] H. R. Ueda, M. Hagiwara and H. Kitano, J. Theor. Biol. **210**, 401 (2001).
[3] D. B. Forger and C. S. Peskin, Proc. Natl. Acad. Sci. USA **100**, 14806 (2003).
[4] S. M. Reppert and D. R. Weaver, Nature **418**, 935 (2002).
[5] L. Glass and M. C. Mackey, *From Clocks to Chaos: The Rhythms of Life*, Princeton: Princeton University Press, (1988).

ISSN 1003-7713/DOI:10.1360/cjcp2007.20(2).119.7

[6] P. Smolen, D. A. Baxter and J. H. Byrne, Biophys. J **83**, 2349 (2002).
[7] N. Preitner, F. Damiola, L. Lopez-Molina, J. Zakany, D. Duboule, U. Albrecht and U. Schibler, Cell **110**, 251 (2002).
[8] M. B. Elowitz, A. J. Levine, E. D. Siggia and P. S. Swain, Science **297**, 1183 (2002).
[9] H. H. McAdams, A. Arkin, Proc. Natl. Acad. Sci. USA **94**, 814 (1997).
[10] J. Paulson, Nature **427**, 415 (2004).
[11] J. Hasty, D. McMillen, F. Isaacs and J. J. Collins, Nat. Rev. Genet. **2**, 268 (2001).
[12] R. Bundschuh, F. Hayot and C. Jayaprakash, J. Theo. Biol. **220**, 261 (2003).
[13] J. Paulsson, O. G. Berg and M. Ehrenberg, Proc. Natl. Acad. Sci. USA **97**, 7148 (2000).
[14] J. M. G. Vilar, H. Y. Kueh, N. Barkai and S. Leibler, Proc. Natl. Acad. Sci. USA **99**, 5988 (2002).
[15] T. B. Kepler and T. C. Elston, Biophys. J. **81**, 3116 (2001).
[16] H. H. McAdams, A. Arkin, Trend Genetics **15**, 65 (1999).
[17] J. Hasty, J. Pradines, M. Dolnik and J. J. Collins, Proc. Natl. Acad. Sci. USA **97**, 2075 (2000).
[18] T. S. Gardner, C. R. Cantor and J. J. Collins, Nature **403**, 339 (2000).
[19] H. Kobayashi, M. Kærn, M. Araki, K. Chung, T. S. Gardner and C. R. Cantor and J. J. Collins, Proc. Natl. Acad. Sci. USA **101**, 8414 (2004).
[20] M. B. Elowitz and S. Leibler, Nature **403**, 335 (2000).
[21] O. G. Berg, J. Paulsson and M. Ehrenberg, Biophys. J. **79**, 2944 (2000).
[22] P. Jung and J. W. Shuai, Europhys. Lett. **56**, 29 (2001).
[23] J. W. Shuai and P. Jung, Phys. Rev. Lett. **88**, 068102 (2002).
[24] J. W. Shuai and P. Jung, Proc. Natl. Acad. Sci. USA **100**, 506 (2003).
[25] Z. H. Hou and H. W. Xin, J. Chem. Phys **119**, 11508 (2003).
[26] J. Q. Zhang, Z. H. Hou and H. W. Xin, ChemPhysChem **5**, 1041 (2004).
[27] Z. W. Wang, Z. H. Hou and H. W. Xin, Chem. Phys. Lett. **401**, 307 (2005).
[28] S. Becker-Weimann, J. Wolf, H. Herzel and A. Kramer, Biophys. J. **87**, 3023 (2004).
[29] D. T. Gillespie, J. Phys. Chem. **81**, 2340 (1977).
[30] D. T. Gillespie, J. Chem. Phys. **115**, 1716 (2001).
[31] D. T. Gillespie, J. Chem. Phys. **113**, 297 (2000).
[32] P. Hänggi, ChemPhysChem **3**, 285 (2002).
[33] L. Gammaitoni, P. Hänggi, P. Jung and F. Marchesoni, Rev. Mod. Phys. **70**, 223 (1998).

ISSN 1003-7713/DOI:10.1360/cjcp2007.20(2).119.7